

# Study of Tm:Sc<sub>2</sub>SiO<sub>5</sub> laser pumped into the <sup>3</sup>H<sub>6</sub>–<sup>3</sup>F<sub>4</sub> transition of Tm<sup>3+</sup> ions

Yu.D. Zavartsev, A.I. Zagumennyi, Yu.L. Kalachev, S.A. Kutovoi, V.A. Mikhailov, I.A. Shcherbakov

**Abstract.** The Tm<sup>3+</sup>:Sc<sub>2</sub>SiO<sub>5</sub> crystals of optical quality are grown by the Czochralski method. Lasing at a wavelength of ~1.98 μm is obtained in an active element made of a grown crystal under pumping by an erbium Raman fiber laser at a wavelength of 1.678 μm. The slope efficiency of the laser reaches 42% at an output power up to 320 mW.

**Keywords:** Tm:SSO, Sc<sub>2</sub>SiO<sub>5</sub>, laser pumping, luminescence, lasing.

## 1. Introduction

Diode-pumped two-micron solid-state lasers based on various crystalline matrices doped with thulium ions Tm<sup>3+</sup> are used for solving a wide range of scientific and applied problems in medicine, laser location, and so on [1–3]. These lasers have a high efficiency (~50%) and a high average output power (exceeding 100 W) [4]. However, in spite of the achieved progress, investigations aimed at further improvement in the characteristics of diode-pumped thulium lasers are continued. First of all, these investigations include the search for new crystalline matrices for active elements with new properties extending the field of application of these lasers. One of these new materials for active elements is the Tm<sup>3+</sup>:Sc<sub>2</sub>SiO<sub>5</sub> (Tm:SSO) crystal. This crystal of laser quality was grown and studied for the first time in [5, 6] in order to check the possibility of lasing in this crystal under diode pumping at the wavelength  $\lambda = 0.792 \mu\text{m}$ , which corresponds to the absorption at the <sup>3</sup>H<sub>6</sub>–<sup>3</sup>F<sub>4</sub> transition (Fig. 1).

Lasing in the Tm:SSO crystal pumped by a Ti:sapphire laser at  $\lambda = 0.785 \mu\text{m}$  was demonstrated in [7]. In an active element cooled to 12 °C, the authors obtained a cw output power of ~500 mW with an efficiency of 29% with respect to the absorbed pump power.

One of the new possibilities of improving the characteristics of thulium lasers is to pump Tm:SSO lasers by quasi-resonant radiation with a wavelength of ~1.7 μm, which corresponds to the absorption at the <sup>3</sup>H<sub>6</sub>–<sup>3</sup>F<sub>4</sub> atomic transition (Fig. 1). As was shown on the example of the Tm:YLF crystal in [8], this pumping has a number of advantages. In par-

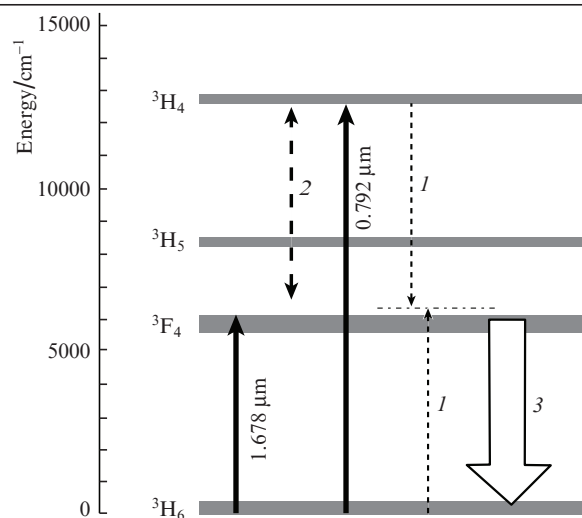


**Figure 1.** Energy level diagram of Tm<sup>3+</sup> ions. The wavelengths of a fibre Raman erbium laser (1.678 μm) and a laser diode (0.792 μm) used for its pumping are shown near the corresponding arrows. The other arrows show (1) cross-relaxation, (2) up-conversion, and (3) lasing.

ticular, the laser retains its high efficiency in a wide range of Tm<sup>3+</sup> concentrations, which is impossible when using diode pumping at  $\lambda \sim 0.8 \mu\text{m}$ .

In the present work, we obtained and studied lasing of a Tm:SSO laser under pumping into the <sup>3</sup>H<sub>6</sub>–<sup>3</sup>F<sub>4</sub> atomic transition for the first time to our knowledge. We also studied the spectral and luminescent properties of active elements under these conditions.

## 2. Laser crystals

The Tm:SSO crystals were grown by the Czochralski method from an iridium crucible [6]. The concentration of Tm<sup>3+</sup> ions in the active elements was ~4%. In experiments, we used active elements of a cubic shape (Fig. 2) with an edge length of 3.5 mm. The opposite faces of the crystals were polished using deep grinding and polishing technique with a parallelism of ~15". The edges of the active elements were X-ray oriented along the X and Y crystallographic axes (Fig. 2). The Z axis lied in a plane perpendicular to the Y axis and was inclined at ~121° to the X axis. The active element was attached by its flat planes to copper heat sink plates with a good thermal contact. The crystal faces were not coated with anything.

Yu.D. Zavartsev, A.I. Zagumennyi, Yu.L. Kalachev, S.A. Kutovoi, V.A. Mikhailov, I.A. Shcherbakov A.M. Prokhorov General Physics Institute, Russian Academy of Sciences, ul. Vavilova 38, 119991 Moscow, Russia; e-mail: kalachev@kapella.gpi.ru

Received 19 February 2013; revision received 23 April 2013  
Kvantovaya Elektronika 43 (11) 989–993 (2013)  
Translated by M.N. Basieva

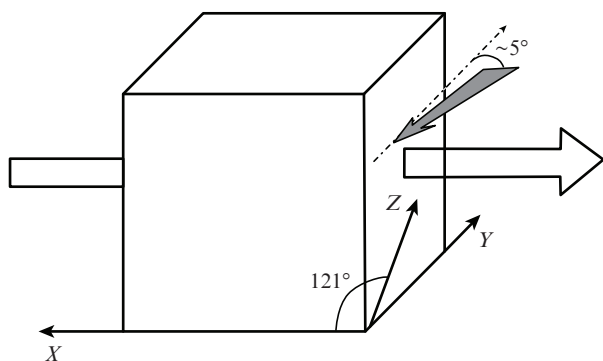


**Figure 2.** Schematic of the mutual orientation of the  $X$ ,  $Y$ , and  $Z$  crystallographic axes and the pump and laser beams. The shaded arrow shows the pump beam direction (almost grazing incidence on the exit face of the crystal) in the measurements of luminescence.

### 3. Spectral and luminescent characteristics

The absorption spectra of the Tm:SSO crystal within the range 0.3–2.3  $\mu\text{m}$  (Fig. 3) were studied using a Shimadzu UV-3600 spectrophotometer. The linearly polarised radiation of the fibre pump laser at a wavelength of 1.678  $\mu\text{m}$ , which does coincide with the absorption maximum, is rather strongly ( $\sim 50\%$ ) absorbed in the active element for both polarisation directions.

The luminescence spectra of the Tm:SSO active element were measured on an MDR-204 monochromator with a Hamamatsu G5852 photodiode. The pump radiation at  $\lambda = 1.678 \mu\text{m}$  in the form of a parallel beam  $\sim 0.5 \text{ mm}$  in diameter was laterally incident on the crystal face perpendicular to the  $X$  axis at a small angle (smaller than  $5^\circ$ ) to the  $Y$  axis. Therefore, we had almost grazing incidence of pump radiation on the crystal face with a small depth of its penetration into the crystal and, hence, only a slight distortion of the luminescence spectra due to the absorption in the crystal. We recorded the luminescence propagating along the  $X$  axis. The pump radiation polarisation was vertical in all the experiments.

The crystal luminescence was observed in the range 1.6–2.1  $\mu\text{m}$  (Fig. 4). The luminescence component polarised perpendicular to the pump polarisation plane was most intense. The spectra of both components had a similar shape. The pump radiation spectrum consists of two lines, with  $\lambda = 1.55$  and 1.678  $\mu\text{m}$  (Fig. 4). The most part of the pump power (more than 90%) belongs to the line with  $\lambda = 1.678 \mu\text{m}$ , and the absorption coefficient at this wavelength is also considerably higher, because of which we can conclude that the contribution made to the excitation by radiation with  $\lambda = 1.55 \mu\text{m}$  is negligibly small.

We also observed a luminescence band in the region of 0.8  $\mu\text{m}$ , which corresponds to the  ${}^3\text{H}_6\text{--}{}^3\text{H}_4$  transition. The  ${}^3\text{H}_4$  level is populated both as a result of the cross-relaxation process  ${}^3\text{F}_4 + {}^3\text{F}_4 \rightarrow {}^3\text{H}_6 + {}^3\text{H}_4$  and due to the absorption of pump radiation photons by excited ions in the  ${}^3\text{F}_4$  state. The absorption from the excited state is possible in the case of additional participation of crystal lattice phonons. Therefore, some portion of the pump radiation is uselessly spent on this process, which decreases the two-micron laser efficiency. This feature is also typical for other thulium lasers. Noticeable

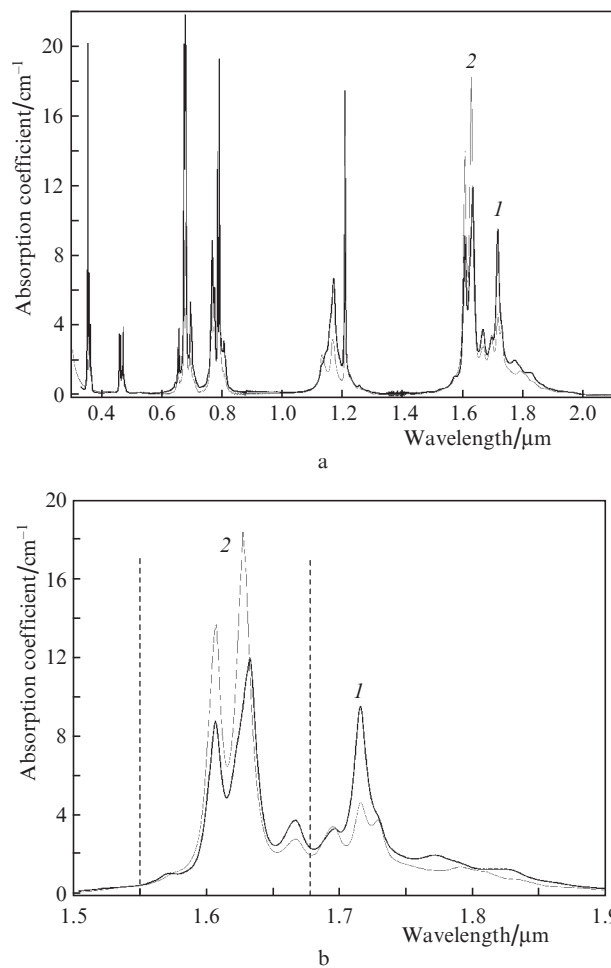


**Figure 3.** Absorption spectra in the Tm:SSO crystal for radiation propagating along the  $X$  axis with (1) parallel and (2) perpendicular polarisation with respect to the  $Y$  axis. The dashed lines denote the wavelengths of the pump erbium fibre laser without (1.55  $\mu\text{m}$ ) and with (1.678  $\mu\text{m}$ ) Raman conversion.

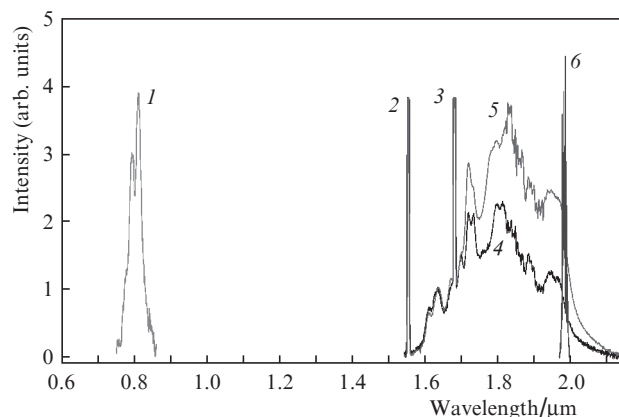


**Figure 4.** Luminescence spectra of the Tm:SSO crystal in the case of propagation along the  $X$  axis with the polarisation oriented (5) parallel and (4) perpendicular to the  $Y$  axis; small admixture of unconverted radiation of the pump erbium fibre laser (2); main part of the pump radiation passed through the Raman converter (3), and laser spectrum (6). The spectral line (1) appears due to the up-conversion in the SSO crystal.

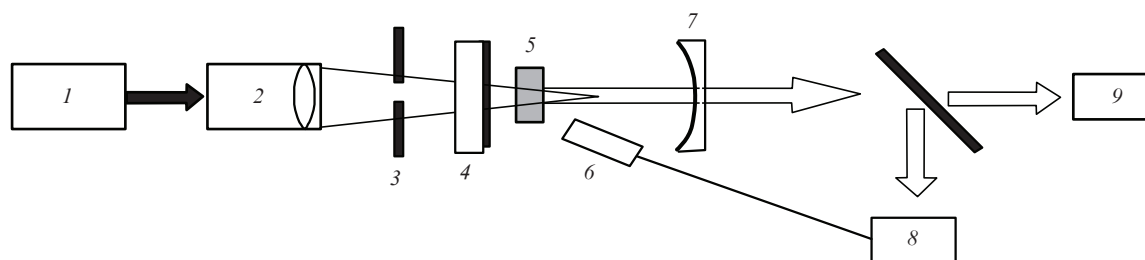


**Figure 5.** Schematic of the experimental setup: (1) pump laser; (2) focusing lens; (3) mechanical chopper; (4) dichroic mirror; (5) active element; (6) fibre tip; (7) output mirror; (8) monochromator; (9) power meter.

luminescence observed at  $\lambda = 1.65 \mu\text{m}$  is also occurs due to up-conversion processes.

#### 4. Laser experiments

The scheme of the experimental setup is shown in Fig. 5. The nearly semi-concentric cavity of the laser was formed by a plane dichroic input mirror with the reflection coefficient  $R \approx 100\%$  for the laser wavelength  $1.98 \mu\text{m}$  and a concave spherical output mirror with a curvature radius of  $52 \text{ mm}$  and  $R = 95\%$  at  $\lambda \approx 1.98 \mu\text{m}$ . In most experiments, the active element was oriented so that the  $X$  axis was directed along the cavity axis and the  $Y$  axis was horizontal.

Pumping was performed by an erbium fibre laser with Raman frequency conversion emitting at  $\lambda = 1.678 \mu\text{m}$  (the same as in [8]). The beam quality of the single-mode linearly polarised pump laser radiation was close to the Gaussian beam quality ( $M^2 \sim 1$ ). The polarisation plane of pump radiation was oriented vertically. The pump spot diameter in the active element was variable within the range  $\sim 15\text{--}100 \mu\text{m}$  by moving a lens with a focal distance of  $80 \text{ mm}$ . This ensured a good coincidence of the pump spot diameter with the transverse size of the fundamental cavity mode and, hence, created the optimal conditions for achieving the highest laser efficiency. The optimal pump spot diameter was  $\sim 80 \mu\text{m}$ .

The pulsed pump regime was obtained using a mechanical rotating chopper (3) (Fig. 5) placed between the lens focusing the pump beam and the highly reflecting mirror. The ratio of the open time of the chopper to its rotation period was  $1:20$ . The chopper rate was  $\sim 10 \text{ s}^{-1}$ . In the case of pulsed pumping, the effect of heating of the active element in the pumped region on the laser characteristics was almost completely eliminated. To determine the absorbed pump power, we measured the total (pump and laser) power immediately behind the output mirror and subtracted from it the laser power measured behind an optical filter (Ge plate) cutting the pump radiation. In the experiments, we used an Ophir Nova II power meter. The power measurement error did not exceed  $5\%$ .

Lasing in the Tm:SSO crystal under pulsed pumping at  $\lambda = 1.678 \mu\text{m}$  was obtained when the absorbed power exceeded the threshold value of  $\sim 180 \text{ mW}$  (Fig. 6). The laser radiation was linearly polarised parallel to the  $Y$  axis. With increasing pump power to  $\sim 600 \text{ mW}$ , the output laser power increased almost linearly. The slope efficiency of the laser reached  $42\%$ . With a further increase in the pump power, the slope efficiency slightly decreased. The highest achieved output power was  $320 \text{ mW}$  at a pump power of  $980 \text{ mW}$ . Thus, the optical laser efficiency was  $33\%$ . It should be noted that the experimental efficiencies of the Tm:SSO laser under pumping at  $\lambda = 1.678 \mu\text{m}$  are slightly lower than the best efficiencies of other

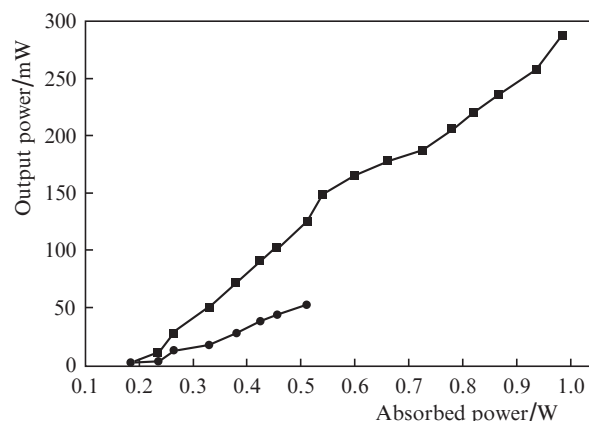


**Figure 6.** Dependences of the Tm:SSO laser output power on the absorbed pump power in the cw (●) and pulsed (■) regimes. The  $X$  axis of the Tm:SSO crystal is oriented along the optical axis of the laser cavity.

diode-pumped thulium lasers. This fact indicates that the Tm:SSO crystal quality is sufficiently good but still lower than the quality of widely used Tm:YAG, Tm:YLF, and other thulium crystals. On the other hand, this result confirms our expectations of a high efficiency of pumping at  $\lambda = 1.678 \mu\text{m}$ .

We also studied the operation of the Tm:SSO laser under cw pumping. The excitation threshold was almost the same as in the case of pulsed pumping ( $220 \text{ mW}$ ). However, the laser efficiency was much lower. At a pump power of  $500 \text{ mW}$ , the output laser power was  $60 \text{ mW}$  (optical efficiency  $13\%$ ), which is approximately twice as low as in the case of pulsed pumping. The slope efficiency was  $19\%$ .

Laser radiation was also obtained when the  $Y$  axis of the crystal was oriented along the cavity axis. The  $X$  axis in this case was directed horizontally. The output laser characteristics are presented in Fig. 7. In this case, the lasing threshold is considerably higher, of about  $450 \text{ mW}$ . Correspondingly, the laser efficiency decreases. The highest output power achieved under pulsed pumping was  $160 \text{ mW}$  with an optical efficiency of  $\sim 16\%$ , which is approximately twofold lower than when the  $X$  axis of the crystal was oriented along the cavity axis. The slope efficiency was  $\sim 29\%$ .

The output laser power achieved under cw pumping was up to  $30 \text{ mW}$ . The lasing efficiency in this case was only  $\sim 4\%$  at a slope efficiency of  $\sim 13\%$ .

The experiments show that the laser efficiency considerably decreases when the  $Y$  axis is oriented along the cavity axis. This can be explained by strongly different gains for radiation propagating along the  $X$  and  $Y$  axes. In addition, it

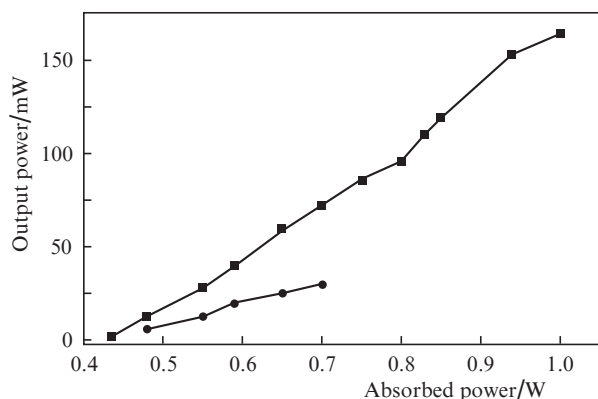


**Figure 7.** Dependences of the Tm:SSO laser output power on the absorbed pump power in the cw (●) and pulsed (■) regimes. The Y axis of the Tm:SSO crystal is oriented along the optical axis of the laser cavity.

is very probable that the crystal structure in the direction of the X axis is more perfect.

The Tm:SSO laser spectrum was studied at different pump powers in the case when the X axis of the active element was directed along the cavity axis (Fig. 8). At high pump powers, the spectrum has a shape of a broad band extended from  $\sim 1.973$  to  $\sim 1.991$   $\mu\text{m}$ . With decreasing pump power, the spectral width decreases to  $\sim 15$  nm, while the spectral shape almost does not change. The irregular structure of the spectrum is caused by the presence of selective units in the cavity, namely, Fabry–Perot interferometers formed by the active element faces without antireflection coating, as well as by these faces and the plane highly reflecting mirror. It should be noted that the spectral width of the Tm:SSO laser radiation is one of the largest spectral widths among thulium lasers. In addition, the lifetime of the excited state of  $\text{Tm}^{3+}$  ions in this crystal is rather short (1.14 ms [9]) comparatively to the other thulium-doped crystals. These two features of the Tm:SSO crystal are favourable for stable generation of ultra-short laser pulses in the mode-locking regime.

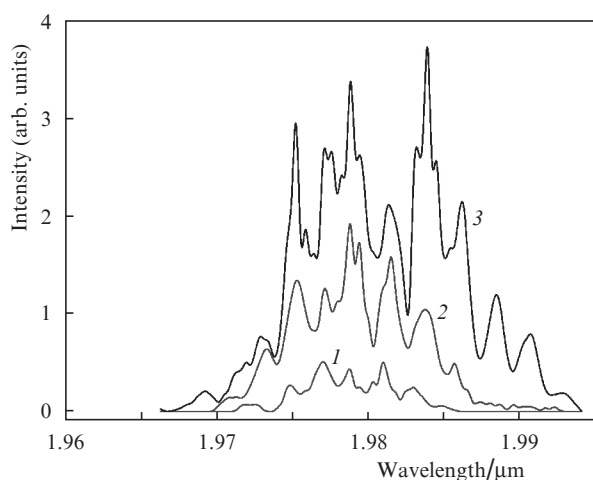


**Figure 8.** Spectrum of the Tm:SSO laser at absorbed pump powers of (1) 0.25, (2) 0.5, and (3) 1 W.

The experiments showed that the luminescence intensity from the pumped region of the crystal depends on the occurrence of lasing in this region. In this connection, we measured the luminescence intensity at a wavelength of  $\sim 0.8$   $\mu\text{m}$  (up-conversion luminescence) and at the lasing wavelength  $\lambda \sim 1.98$   $\mu\text{m}$ . The end of a quartz fibre 600  $\mu\text{m}$  in diameter was placed at a minimal distance from the active element surface at a small angle to the cavity axis in the direct vicinity of the pumped region without blocking it [see unit (6) in Fig. 5]. Radiation propagated through the fibre to the monochromator slit. In these experiments, lasing was interrupted by introducing a nontransparent screen in the cavity near the output mirror. The pump paths remained unchanged.

The luminescence intensity at  $\lambda = 1.98$   $\mu\text{m}$  was found to increase when lasing occurred. An inverse dependence was observed for luminescence at  $\lambda = 0.8$   $\mu\text{m}$ , i.e., the luminescence intensity was higher in the absence of lasing.

The difference between the luminescence intensities in the cases with and without lasing reached 15%–30%. The largest changes (to 30%) were observed in the long-wavelength spectral range (1.7–2.1  $\mu\text{m}$ ). The structure of the luminescence spectrum almost did not depend on the experimental conditions.

## 5. Conclusions

The main result of this work is the attainment of lasing in the Tm:SSO crystal with a rather high (for thulium lasers) efficiency of 42% under pumping at  $\lambda = 1.678$   $\mu\text{m}$ .

The studied crystal demonstrated anisotropy of laser and luminescent properties at orientation of the X or Y crystallographic axes along the cavity axis. The luminescence intensity and the lasing efficiency for these two directions differ approximately by one and half–two times, while the absorption coefficient at the pump wavelength changes less than by 15%.

The laser efficiency in the cw regime was considerably lower. This can be explained by a strong heating of the active element in the pumped region, which induces additional losses due to absorption under the conditions of a quasi-three-level lasing scheme. The high losses of radiation in the crystal can also be caused by the imperfect crystal growth technology and, in particular, by the formation of short-lived colour centres.

Thus, despite the success achieved in improving the laser characteristics of the Tm:SSO crystal since our first experiments with diode pumping [6], the optical quality of this crystal still needs further improvement. The main criterion of a high quality of Tm:SSO laser crystals will be an increase in the cw laser efficiency.

## References

1. Jelinkova H., Koranda P., Sulc J., Nemeč M., Černý P., Pasta J. *Proc. SPIE Int. Soc. Opt. Eng.*, **6871**, 68712N (2008).
2. Henderson S.W., Suni P.J.M., Hale C.P., Hannon S.M., Magee J.R., Burns D.L., Yuck E.H. *IEEE Trans. Geosci. Remote Sens.*, **31** (1), 4 (1993).
3. Zadeh M.E., Sorokina I.T. (Eds) *Mid-Infrared Coherent Sources and Application* (Berlin: Springer, 2008) pp 575–588; <http://www.springer.com/engineering/book/978-1-4020-6439-5>.
4. Lai K.S., Phna P.B., Wu R.F., Lan E., Toh S.W., Toh B.T., Chug A. *Opt. Lett.*, **25** (21), 1591 (2000).

5. Kalachev Yu.L., Zavartsev Yu.D., Zagumennyi A.I., Kutovoi S.A., Mikhailov V.A., Podreshetnikov V.V., Shcherbakov I.A. *Abstr. of 19th Int. Conf. on Advanced Laser Technologies (ALT'11)* (Golden Sands, Bulgaria, 2011) p. 87.
6. Zavartsev Yu.D., Zagumennyi A.I., Kalachev Yu.L., Kutovoi S.A., Mikhailov V.A., Podreshetnikov V.V., Shcherbakov I.A. *Kvantovaya Elektron.*, **41** (5), 420 (2011) [*Quantum Electron.*, **41** (5), 420 (2011)].
7. Xu J., Zheng L.H., Yang K.J., Dekorsy T., Wang Q.G., Xu X.D., Su L.B. *Tech. Dig. Conf. on Advances in Optical Materials* (San Diego, Cal., USA, 2012) pp 1–3; <http://dx.doi.org/10.1364/AIOM.2012.IW3D.1>.
8. Kalachev Yu.L., Mikhailov V.A., Podreshetnikov V.V., Shcherbakov I.A. *Opt. Commun.*, **284**, 3357 (2011).
9. Zheng L., Xu J., Su L., Li H., Ryba-Romanowski W., Lisieck R., Solarz P. *Appl. Phys. Lett.*, **96**, 121908 (2010).